Development 135, 3291-3300 (2008) doi:10.1242/dev.022871

Insulin receptor substrate 1 is an effector of sonic hedgehog mitogenic signaling in cerebellar neural precursors

Susana R. Parathath[1,*], Lori Anne Mainwaring[1,2,*], Africa Fernandez-L[1], Dane Ohlosson Campbell[1] and Anna Marie Kenney[1,2,3,†]

Sonic hedgehog (SHH) and insulin-like growth factor (IGF) signaling are essential for development of many tissues and are implicated in medulloblastoma, the most common solid pediatric malignancy. Cerebellar granule neuron precursors (CGNPs), proposed cells-of-origin for specific classes of medulloblastomas, require SHH and IGF signaling for proliferation and survival during development of the cerebellum. We asked whether SHH regulates IGF pathway components in proliferating CGNPs. We report that SHH-treated CGNPs showed increased levels of insulin receptor substrate 1 (IRS1) protein, which was also present in the germinal layer of the developing mouse cerebellum and in mouse SHH-induced medulloblastomas. Previous roles for IRS1, an oncogenic protein that is essential for IGF-mediated proliferation in other cell types, have not been described in SHH-mediated CGNP proliferation. We found that IRS1 overexpression can maintain CGNP proliferation in the absence of SHH. Furthermore, lentivirus-mediated knock down experiments have shown that IRS1 activity is required for CGNP proliferation in slice explants and dissociated cultures. Contrary to traditional models for SHH signaling that focus on gene transcription, SHH stimulation does not regulate *Irs1* transcription but rather stabilizes IRS1 protein by interfering with mTOR-dependent IRS1 turnover and possibly affects *Irs1* mRNA translation. Thus, we have identified IRS1 as a novel effector of SHH mitogenic signaling that may serve as a future target for medulloblastoma therapies. Our findings also indicate a previously unreported interaction between the SHH and mTOR pathways, and provide an example of a non-classical means for SHH-mediated protein regulation during development.

KEY WORDS: Sonic hedgehog, Cerebellum, Neural precursor, Insulin-like growth factor, Insulin receptor substrate 1, Proliferation, Mouse

INTRODUCTION

Medulloblastoma is the most common malignant solid tumor in children. These tumors arise in the cerebellum, a region of the brain with important roles in movement, coordination and possibly learning. Traditional treatments for medulloblastomas – radiation, surgery and multi-agent chemotherapy – cause devastating side effects in long-term survivors (Packer et al., 1999), including cognitive decline, psychiatric problems, seizures and movement disorders. The poor understanding of molecular events leading to the formation and maintenance of medulloblastoma has hindered the advancement of treatment options.

CGNPs are proposed cells of origin for some classes of medulloblastoma (Provias and Becker, 1996). After birth (approximately the first 2 weeks in mice), CGNPs undergo a rapid expansion phase in the cerebellar external granule layer (EGL). After this expansion CGNPs migrate through the underlying layer of Purkinje neurons with which they will ultimately form synapses. The mature granule neuron cell bodies localize to the internal granule layer (IGL) (Hatten and Heintz, 1995). Normal CGNP proliferation is dependent upon signaling by both SHH and IGF, which are also implicated in medulloblastomas (Altman and Bayer, 1997; Ho and Scott, 2002; Knoepfler and Kenney, 2006; Marino, 2005; Wetmore, 2003).

[1]Department of Cancer Biology and Genetics, Memorial Sloan-Kettering Cancer Center, New York, NY 10021, USA. [2]Program in Biochemistry, Cell, and Molecular Biology, Weill Cornell Graduate School, New York, NY 10021, USA. [3]Program in Neurobiology, Weill Cornell Graduate School, New York, NY 10021, USA.

*These authors contributed equally to this work
†Author for correspondence (e-mail: kenneya@mskcc.org)

Accepted 28 July 2008

SHH is produced by Purkinje neurons and loss of SHH leads to reduced proliferation in the EGL of neonatal mice (Dahmane and Ruiz-i-Altaba, 1999; Wallace, 1999; Wechsler-Reya and Scott, 1999). Treatment of CGNPs in culture with SHH increases BrdU incorporation (Dahmane and Ruiz-i-Altaba, 1999; Wallace, 1999; Wechsler-Reya and Scott, 1999); however, the mechanisms underlying SHH mitogenic signaling in CGNPs continue to be subject to ongoing investigation. Classic mitogens such as epidermal growth factor (EGF) or platelet-derived growth factors (PDGFs) signal through receptor tyrosine kinases. By contrast, SHH activates a non-receptor tyrosine kinase-associated pathway. In the absence of SHH, the transmembrane protein patched (PTCH1) represses smoothened (SMO), a G-protein coupled receptor-resembling protein (Alcedo et al., 1996). When SHH binds to PTCH1, SMO is released from inhibition and the pathway is activated, resulting in activation of target genes including *Ptch1* itself, as well as the transcription factors *N-myc* (*Mycn* – Mouse Genome Informatics) *Gli2* and *Gli1*, a target of GLI2 (Ho and Scott, 2002). SHH signaling during cerebellar development occurs primarily through the activation of GLI2; mutations in GLI2 result in abnormal CGNP proliferation, as well as foliation defects (Corrales et al., 2006; Corrales et al., 2004).

Traditional receptor tyrosine kinase signaling mediated by IGF family members has roles in CGNP proliferation and SHH-associated medulloblastomas. IGF1 and IGF2 are expressed in the developing and mature cerebellum. Activation of the IGF pathway is found in medulloblastomas (Reiss, 2002), and IGF2 in particular is required for SHH-mediated medulloblastoma formation (Hahn et al., 2000) *in vivo* and medulloblastoma cell proliferation *in vitro* (Hartmann et al., 2005). IGF1 and IGF2 activate the IGF receptor. One way through which IGF-mediated phosphoinositide-3 kinase (PI-3K) signaling cooperates with SHH signaling is by inhibiting GSK3β (Kenney et al., 2004; Mill et al., 2005), which blocks cell cycle progression in CGNPs by phosphorylating N-myc and targeting it to the proteosome for

degradation. The goal of our current study is to identify additional mechanisms through which SHH and IGF pathway members cooperate to promote CGNP proliferation.

IGF binding to its receptor leads to tyrosine phosphorylation of scaffolding proteins that act as downstream effectors, including GAB1 and IRS1-IRS4 (Van Obberghen et al., 2001). Tyrosine phosphorylation of IRS proteins provides multimeric docking sites for Src homology 2 (SH2) domain-containing proteins. Through this mechanism IRS1-IRS4 and GAB1 can activate PI-3K (White, 1998), which executes many of the functions of insulin-like growth factors. However, in addition to their overlapping ability to activate PI-3K, IGF effectors also have unique effects on cell survival, proliferation and differentiation. In particular functional IRS1 is essential for the proliferative effects of the IGF receptor (Waters et al., 1993). Aberrant IRS1 expression has been associated with several types of human cancer, including medulloblastoma (Del Valle et al., 2002; Waters et al., 1993), and its overexpression can drive mammary tumor formation in mice (Dearth et al., 2006). The role of IRS1 in neural precursor expansion, however, is poorly understood.

We asked whether SHH treatment alters expression or activity of IGF pathway effectors. Interestingly, we observed no effect of SHH on AKT activity, in contrast to a previous report from a cell line (Riobo et al., 2006). Among IGF receptor substrates we investigated, only IRS1 protein levels were increased in the presence of SHH. In neonatal mouse cerebella, we detected IRS1 protein in the germinal layer of the developing cerebellum. Lentivirus-mediated IRS1 knockdown reduced SHH proliferative effects on CGNPs without affecting survival. Interestingly, our studies indicate that SHH treatment does not alter *Irs1* mRNA expression. Instead, SHH increases IRS1 protein stability by impeding an mTOR (FRAP1 – Mouse Genome Informatics) -dependent turnover process and may also promote *Irs1* mRNA translation. Our results reveal a novel mechanism through which SHH uses components of the IGF pathway to drive proliferation, as well as providing evidence that SHH signaling directly or indirectly affects the mTOR pathway.

MATERIALS AND METHODS

Animal studies

Harvest of neural precursors from neonates and preparation of cerebella from wild-type and mutant mice for histological analysis were carried out in compliance with the Memorial Sloan-Kettering Institutional animal care and use committee guidelines.

Cerebellar granule neuron precursor culture

CGNP cultures were generated as previously described (Kenney and Rowitch, 2000). Briefly, cerebella from postnatal day (P) 5 Swiss-Webster 129 (SW129) mice were dissected into Hanks buffered saline solutions (HBSS) (Gibco) supplemented with glucose. The meninges were removed and cerebella were pooled and treated with Trypsin-EDTA for dissociation by trituration into HBSS. Triturated cells were centrifuged and resuspended in Dulbecco's modified Eagle's medium-F-12 (DMEM/F12) (Gibco) supplemented with 25 mM KCl, N2 supplement (Gibco), antibiotic and 10% fetal calf serum (Sigma). Cells were plated in individual poly-DL-ornithine (Sigma) pre-coated wells of a six-well plate and for treated samples 3 μg/ml SHH (Biogen) was added to the media. After 6-12 hours the media were changed to DMEM/F12/N2/KCl minus serum, with or without SHH, as indicated. Unless otherwise stated, cells were left undisturbed for 24 hours prior to further treatment or analysis. For purified cultures, resuspended CGNPs were passed through a Percoll gradient as previously described (Wechsler-Reya and Scott, 1999).

Cerebellar slice cultures

Cerebella from P5 pups were aseptically removed and embedded in 3% low-melting agarose (Bio-Rad) made with HBSS. Cerebella were cut using a Leica VT1000S vibratome into 300 μm sections and cultured on Whatman nuclopeore track-etched membrane (Fisher Scientific) in serum-free media for 24 hours supplemented with SHH. After 24 hours, indicated sections were infected with shRNA lentiviruses targeting IRS1 for 6 hours. The slices were maintained in serum free media for 48 hours and pulsed with BrdU for an additional 4 hours. Slices were flash frozen, sectioned and stained for BrdU and DAPI.

Protein preparation and immunobloting

For immunoblot analysis, cells were scraped cells loose into their medium. Cells were washed once in PBS and protein extracts were prepared as previously described (Kenney and Rowitch, 2000). Protein content was determined by using the BioRad protein assay. Assays were performed in duplicate for each sample. Each sample (50 μg) was separated by sodium dodecyl sulfate-polyacrylamide gel electrophoresis (SDS-PAGE) on 8% polyacrylamide gels and then transferred in 20% methanol buffer at 4°C to Immobilon polyvinylidene difluoride (Millipore) membranes. Standard western blot procedures (see Kenney and Rowitch, 2000) were used to determine protein levels. Antibodies used for western blotting were: IGFRβ, N-myc and cyclin D2 (Santa Cruz), IRS1, IRS2, phosphorylated IRS1 (S636/639), phosphorylated AKT (S473), AKT, GAB1, phosphorylated ERK, phosphorylated p70S6 kinase (T389), phosphorylated ribosomal protein S6 (S235/236) (Cell Signaling) and β-tubulin (Sigma). Peroxidase activity was detected using Amersham's ECL reagents and exposing membranes to Kodak Biomax film. Multiple exposures were taken to avoid saturating film. The film was scanned and the digitalized images were quantified by densitometry using Adobe Photoshop 9.0 software.

Immunofluorescence

Frozen sections (10 μm) from SW129 pups were dried and then boiled in 0.01 M citric acid for 15 minutes for antigen retrieval. For paraffin-embedded sections, tissues were first de-waxed and re-hydrated prior to antigen retrieval. After cooling, slides were washed twice with PBS for 10 minutes. Sections were blocked with 10% normal goat serum (Sigma) in 0.25% Triton X-100/PBS for 1 hour at room temperature. Primary antibodies for IRS1 (Cell Signaling), GFAP (Cell Signaling), BrdU (Becton Dickinson) and Ki67 (Vector Laboratories) were added to the blocking solution at a 1:100 dilution and incubated overnight at 4°C. After washing in PBS, slides were incubated with either goat anti-rabbit or goat anti-mouse fluorescently tagged secondary antibody (Invitrogen) at a 1:5000 dilution for 1 hour at room temperature. Sections were mounted using Vectashield mounting media with DAPI (Vector Laboratories).

For detecting BrdU incorporation, dissociated CGNPs were grown on poly-DL-ornithine-coated glass coverslips. Cells were pulsed with 20 μg/ml BrdU for 2 hours. The cells were fixed with 4% paraformaldehyde for 20 minutes followed by two 10-minute washes with PBS. The coverslips were treated with 2 N HCl for 2 minutes followed by two 10-minute washes with PBS. Cells were blocked for 30 minutes then exposed to primary and secondary antibodies according to standard methods (details can be provided on request). All other antibodies, IRS1 (Cell Signaling or Upstate), Ki67 (Vector Laboratories), p27 (BD Pharmingen), PCNA (Calbiochem), ZIC1 (gift from Rosalind Segal, Harvard) and cleaved caspsase 3 (Cell Signaling) were used at a 1:100 dilution in blocking solution.

Reverse transcriptase and quantitative PCR

RNA from CGNPs was collected using TRIZOL reagent according to the manufacturer's instructions. RNA samples were resuspended in 87.5 μL DEPC-treated water. In order to remove fully any residual DNA from the samples, RNA was further purified using the RNeasy Mini Kit (Qiagen) according to manufacturer's instructions. DNase (Qiagen) digestion was performed in solution prior to further RNA purification over the RNeasy column.

A 50 μl reaction volume was used for 50 ng RNA of each sample using SuperScriptOne-Step RT-PCR with Platinum Taq (Invitrogen). Samples were run as per manufacturer's instructions. Absence of genomic DNA was verified by omitting the RT step and using Taq alone. Primer sequences were as follows: β-actin sense, 5′-CACAGCTACAAAGAGCGGCTCCACC-3′; β-actin antisense, 5′-CACTGCATTCTAGTTGTGGTTTGTCC-3′; cyclin D2 sense, 5′-CACTTCCTCTCCAAAATGCCA-3′; cyclin D2 antisense, 5′-CCTGGCGCAGGCTTGACTC-3′; IRS1 sense, 5′-CCCGCGTTCAAG-

GAGGTCTG-3′; IRS1 antisense, 5′-TGGCTGGGTGGAGGGTTGTT-3′; GLI1 sense, 5′-CCACGGGGAGCGGAAGGAA-3′; GLI1 antisense, 5′-AGGCGGCGAAGCGTGGAGAGT-3′; GLI2 sense, 5′-AGCCCCTG-CACTGGAGAAGAAAGA-3′; GLI2 antisense, 5′-CTGGGGCTGCGA-GGCTAAAGAG-3′; N-myc sense, 5′-GCCTTCTCGTTCTTCACCAG-3′; N-myc antisense, 5′-GCGGTAACCACTTTCACGAT-3′. PCR products were resolved on a 2.5% agarose-ethidium bromide gel.

For quantitative PCR, total mRNA was extracted from untreated and SHH-treated CGNP cultures as described above. cDNA was generated with SuperScript First-Strand Synthesis System for RT-PCR (Invitrogen) as per manufacturer's instructions. TaqMan Gene Expression Assays (Applied Biosystems) using TaqMan custom designed MGB probes for IRS1 (Mm01278327_m1) and β-actin (Mm01191484_m1) were performed in triplicate according to the manufacturer's protocol on an ABI 7000 Sequence Detection System. Data were analyzed with ABI GeneAmp SDS software (Applied Biosystems). The average threshold cycle (CT) was determined to quantify initial transcript levels and results reported as fold changes.

Retroviruses

IRS1-expressing retroviruses were constructed by ligating a mouse IRS1 cDNA (gift of Morris White, Harvard) into the retroviral vector pIG. The construct was verified by sequencing. GLI1-expressing retrovirus was provided by Rob Wechlser-Reya (Duke). For producing viruses, 293e packaging cells (Invitrogen) were co-transfected with 10 μg each of retrovirus construct, vsv-g and gagpol plasmids using Fugene in DMEM containing 10% fetal calf serum. Twenty-four hours later, the medium was aspirated and replaced with fresh medium. Viral supernatant was collected for 3 days and stored at 4°C, then pooled and filtered through a 45 μm filter. CGNPs were infected by removing their medium, exposing them to filtered viral supernatants for 2 hours, then replacing with fresh or conditioned medium as appropriate.

Short hairpin RNA lentiviruses

293e packaging cells were co-transfected with lentiviral constructs expressing short hairpin RNAs targeting IRS1 (The RNAi Consortium) or GFP, delta 8.9 and vesicular stomatitis virus G glycoprotein plasmids, using Fugene 6 transfection reagent (Roche). The media was changed 12 hours after transfection and supernatants (10 ml) were harvested every 24 hours for 72 hours and kept at 4°C until they were pooled, filtered through 0.45 μm syringe filters, aliquoted and stored at –80°C until use. CGNPs were infected as described above.

Image capturing

Staining of cultured primary cells and tissue sections was visualized with a Leica DM5000B microscope and images were taken using Leica FW400 software. For quantification of BrdU uptake into newly synthesized DNA, TIFF images of four random fields were taken for each experimental group using the 10× objective. The percentage of cells staining positive for BrdU over the total number of cells was determined using Image Pro Plus software (MediaCybernetics). Confocal images were visualized with Leica TCS AOBS SP2 (Inverted Stand) and images captured with Leica LCS Lite software.

Statistics

Statistical analysis was performed using one-way ANOVA followed by a Bonferroni-Dunn test for multiple comparisons within a group, or a two-tailed *t*-test for comparisons between groups, as indicated by the figure legends; $P<0.05$ was considered significant and is marked by an asterisk. All results are given as mean±s.e.m. Experiments in vitro were performed at least three times, with separate litters of mice, to confirm reproducibility and consistency.

RESULTS

SHH treatment upregulates IRS1 protein levels in CGNPs

In order to determine whether expression levels or activity of IGF pathway components are altered in CGNPs induced to proliferate by SHH in comparison with levels in differentiating (vehicle-treated) CGNPs, we established CGNP primary cultures from PN 5 SW129 mice and treated them with vehicle (PBS) or added SHH to the media for 24 hours. We then prepared protein lysates and used western blot analysis to assess levels of IGF receptor substrates and AKT phosphorylation, a downstream target of PI-3K (Fig. 1A). We also examined levels of cyclin D2, a well-established marker for SHH-induced CGNP proliferation, and ERK phosphorylation, which is known to be unaffected by SHH treatment in CGNPs (Kenney and Rowitch, 2000). We found that SHH-treated CGNPs showed increased levels of IRS1 protein, and that IGF receptor, IRS2 or GAB1 levels did not change in response to SHH (Fig. 1A). IRS1 upregulation correlates with increased cyclin D2 expression. It has been reported that SHH treatment of a fibroblast cell line results in modestly increased phosphorylation of AKT (Riobo et al., 2006). By contrast, we detected no changes in AKT phosphorylation in SHH-treated CGNPs (Fig. 1A, Fig. 4A, Fig. 5A) suggesting functions for IRS1 in CGNPs in addition to its AKT-activating role. The upregulation of IRS1 is also accompanied by activation of IRS1 as seen by its tyrosine phosphorylation, which occurs when the IGF receptor is bound by ligand (Van Obberghen et al., 2001) (see Fig. S1 in the supplementary material).

We next asked whether maintenance of increased IRS1 levels requires ongoing SHH signaling. We treated CGNPs with two well-characterized SHH pathway inhibitors, forskolin and cyclopamine, for increasing lengths of time. Forskolin serves as a potent inhibitor of SHH signaling by increasing cAMP levels, which in turn activates PKA and leads to CGNP cell cycle exit and differentiation (Cai et al., 1999). Cyclopamine is an antagonist of SMO, the activator of SHH signaling (Chen et al., 2002). Treatment with either inhibitor reduced IRS1 and cyclin D2 protein levels in a time-dependent manner (Fig. 1B), with IRS1 loss apparent 6-9 hours after addition of inhibitors. This delayed, rather than immediate, response of IRS1 to SHH inhibition may be a result of the long half-life of IRS1, which has been reported to be up to 10 hours (Lee et al., 2000) or it may suggest that IRS1 is sensitive to cell cycle exit, as CGNPs remain proliferation competent for 6 hours after SHH withdrawal or inhibition (Kenney and Rowitch, 2000).

Recent evidence suggests that IRS1 may have nuclear as well as cytoplasmic functions (Chen et al., 2005; Morelli et al., 2004). To determine the cellular localization of IRS1, we cultured CGNPs on coverslips with or without SHH for 24 hours. We then carried out immunostaining for IRS1 and p27, a predominantly nuclear protein associated with CGNP differentiation (Uziel et al., 2005). As shown in Fig. 1C, SHH-treated CGNP cultures contained populations of cells expressing either p27 (green) or IRS1 (red), and expression of IRS1 and p27 is mutually exclusive in individual cells. When images were merged with blue DAPI (nuclear) staining, we observed IRS1 expression in the nucleus and cytoplasm, which was confirmed by confocal microscopy (Fig. 1C, right panel). These results suggest that IRS1 may perform signaling functions in the cytoplasm, and may also play roles in regulating transcription or DNA repair, nuclear functions previously ascribed to IRS1 (Reiss, 2006; Chen, 2005). The role played by nuclear versus cytoplasmic IRS1 in proliferating CGNPs remains to be determined.

In our hands, mixed CGNP cultures contain up to 10% GFAP-positive cells. Previously, it has been shown that the only SHH-responsive cells and BrdU-incorporating cells in mixed cultures are CGNPs, not those that stain positive for glial markers such as GFAP or O4 (Wechsler-Reya and Scott, 1999). In vivo staining of postnatal day 7 mouse cerebella for GFAP and IRS1 shows that these two

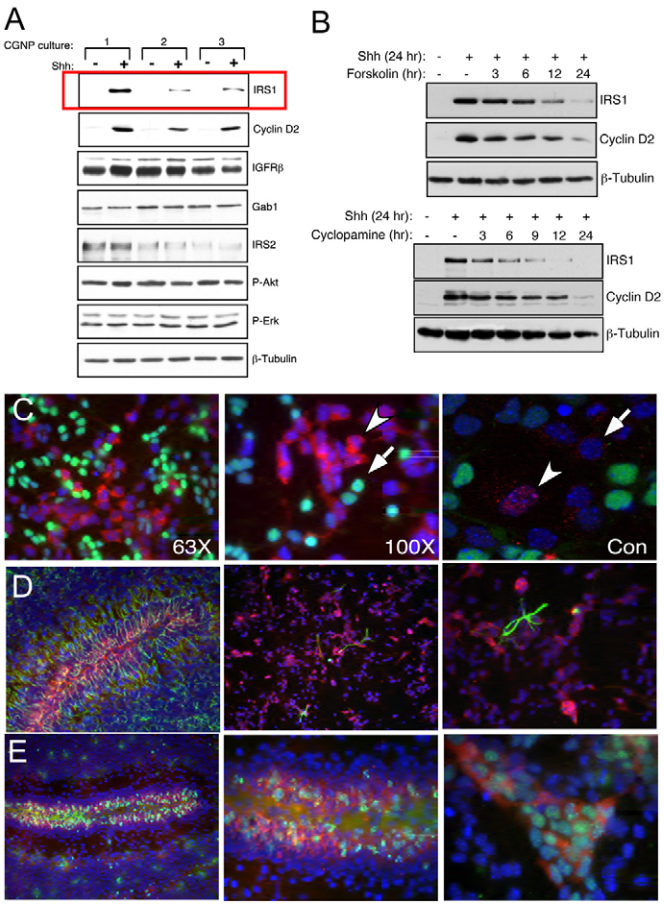

Fig. 1. IRS1 protein is upregulated in proliferating CGNPs. (**A**) CGNP cultures were prepared from different litters on different dates. Preparations of the cells were treated with SHH or left untreated for 24 hours prior to lysis. The autoradiograph depicts a western blot for several downstream components of IGF signaling pathway and the cell cycle progression marker cyclin D2. Only IRS1 levels are upregulated in SHH-treated samples, which correlates with increases in cyclin D2. β-Tubulin demonstrates equal protein loading. (**B**) The autoradiographs show western blots for CGNPs treated with two SHH signaling pathway inhibitors, forskolin (10 μM) or cyclopamine (1 μg/ml), for increasing time points. In the absence of continuous SHH signaling, levels of IRS1 decrease, which also correlates with decreased cyclin D2 expression. (**C**) SHH-treated CGNPs were fixed and immunostained for IRS1 (red) and p27 (green). IRS1 and p27 mark different populations of cells. Confocal imaging (right panel) confirms IRS1 presence in the nucleus (arrowhead) and cytoplasm (arrow). (**D**) Left: cerebellar section from post-natal day 7 mouse immunostained for IRS1 (red) and GFAP (green). Middle (low power) and right (high power): SHH-treated primary CGNP cultures immunostained for IRS1 (red) and GFAP (green). IRS1 is excluded from glia both in vivo and in vitro. (**E**) In the left (low power) and middle (high power) panels, PN 7 mice were pulsed with BrdU and stained for BrdU (green) and IRS1 (red). IRS1 colocalizes to proliferating CGNPs in the EGL. In the far right panel, IRS1 (red) is expressed in the cytoplasm of BrdU-positive cells (green) in CGNP cultures.

markers do not colocalize (Fig. 1D, left panel). To confirm that increased IRS1 expression occurs in CGNPs, not glia, cultures were treated with SHH for 24 hours and then immunostained for GFAP and IRS1 (Fig. 1D, middle and right panels) or BrdU and IRS1 (Fig. 1E, right panel). BrdU-incorporating cells were also Zic1 positive, confirming their identity as CGNPs (see Fig. S2 in the supplementary material). Our results demonstrate that increased IRS1 expression occurs in cells that have incorporated BrdU, both in culture and in vivo, and is excluded from GFAP-expressing glial cells (Fig. 1D,E) (Aruga et al., 2002). Thus, IRS1 is upregulated in proliferating CGNPs.

In vivo, by postnatal day 15 IRS1 levels are reduced, although some expression remains in the EGL in conjunction with the proliferation marker PCNA (see Fig. S2 in the supplementary material). We found that IRS2 was restricted to Purkinje neurons and is excluded from the EGL (see Fig. S2 in the supplementary material). Our observation that IRS2 is not found in CGNPs, but rather located in Purkinje neurons, the cells that provide SHH to CGNPs, suggests that a reported requirement for IRS2 in CGNP proliferation (Schubert et al., 2003) may be attributed to Purkinje cell defects (see Fig. S2 in the supplementary material). Indeed we detected reduced SHH signaling, and reduced levels of IRS1 protein in the EGL of IRS2-null neonatal mouse cerebella (see Fig. S3 in the supplementary material).

SHH signaling stabilizes IRS1 protein levels without altering *Irs1* transcripts

Canonical SHH signaling occurs through the action of GLI and N-myc transcription factors resulting in the upregulation of target mRNA transcripts. In order to determine whether SHH signaling affects IRS1 protein levels by increasing *Irs1* transcripts, we used RT-PCR analysis for *Irs1*, cyclin D2 and actin (Fig. 2A,B). RNA was collected for RT-PCR or quantitative PCR from CGNPs treated with or without SHH for 24 hours. Levels of cyclin D2, an indirect target of SHH signaling (Kenney and Rowitch, 2000) are increased in SHH-treated CGNPs (Fig. 2A). However, levels of *Irs1* are constant regardless of treatment, indicating that SHH does not affect *Irs1* transcription (Fig. 2A,B). These results are in agreement with previous work performed in non-neural cell types showing that IRS1 protein levels can change without changes in *Irs1* transcription (Nemoto et al., 2006; Renstrom et al., 2005; Rice et al., 1993).

To determine whether SHH stabilizes IRS1 protein levels by inhibiting its degradation, we asked how co-treatment of CGNPs with the SHH inhibitor cyclopamine and the proteasome inhibitor lactacystin affected IRS1 protein levels. In the presence of the SHH inhibitor cyclopamine, IRS1 levels declined as expected (Fig. 2C). Reduction in IRS1 protein levels was prevented when lactacystin was also present, suggesting that inhibition of SHH causes IRS1 to be targeted for degradation (Fig. 2C). Moreover, in addition to preventing IRS1 turnover, SHH may also affect *Irs1* mRNA translation, as IRS1 transcripts are present in non-SHH-treated cells but lactacystin treatment did not induce IRS1 protein accumulation, indicating that the *Irs1* mRNA is not being translated in CGNPs that have not been exposed to SHH. However, this remains to be conclusively determined, as current methodologies for examining SHH-responsive mRNA translation have not yet been refined for use with such limited starting material as primary CGNP cultures.

Although SHH signaling does not activate IRS1 transcription, it is possible that the SHH transcriptional target GLI1 can regulate IRS1 protein. To determine whether GLI activity can promote accumulation of IRS1 in CGNPs, we infected CGNP cultures with a GLI1 retrovirus. After the 2 hour infection period, the viral supernatent was withdrawn and replaced with fresh CGNP medium lacking SHH. We examined IRS1 protein levels 36 hours after infection. As shown in Fig. 2D, IRS1 was present in GLI-infected cultures, albeit not at levels as high as in cultures treated with SHH. These results suggest that GLI1 can promote IRS1 protein accumulation, and that there are also GLI-independent mechanisms

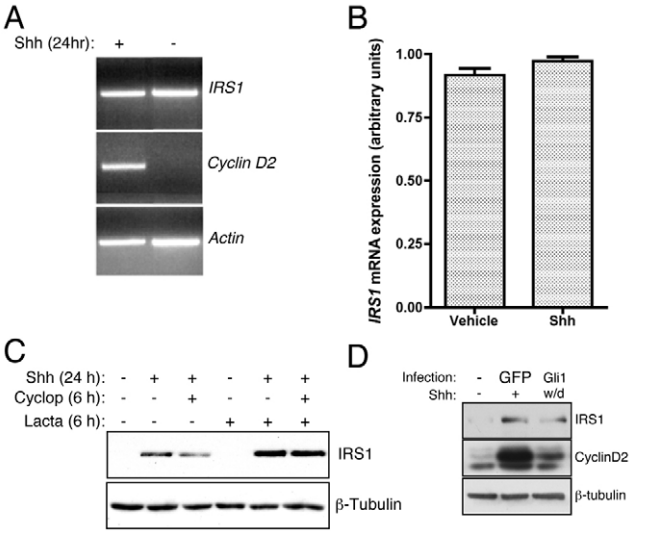

Fig. 2. SHH signaling stabilizes IRS1 protein. (**A**) RNA was collected from SHH-treated CGNPs and RT-PCR analysis was conducted for IRS1, cyclin D2 and β-actin to verify equal RNA input. (**B**) qPCR was used to quantify levels of IRS1 expression. Expression levels of IRS1, depicted as arbitrary units, do not change in response to SHH treatment. (**C**) CGNPs were treated with SHH, cyclopamine or lactacystin (10 μM) for indicated times. Levels of IRS1 protein are stabilized in the presence of the lactacystin and cyclopamine. (**D**) Western blot analysis of IRS1 protein levels in CGNPs infected with GLI1 retroviruses and subsequently cultured without SHH for 36 hours. GLI1 infection can sustain proliferation as indicated by cyclin D2 levels and as previously reported (Oliver et al., 2003). IRS1 was present but at lower levels than in CGNPs infected with GFP-expressing retroviruses and treated with exogenous SHH, suggesting the existence of GLI-mediated and non-GLI-mediated mechanisms that promote IRS1 protein accumulation.

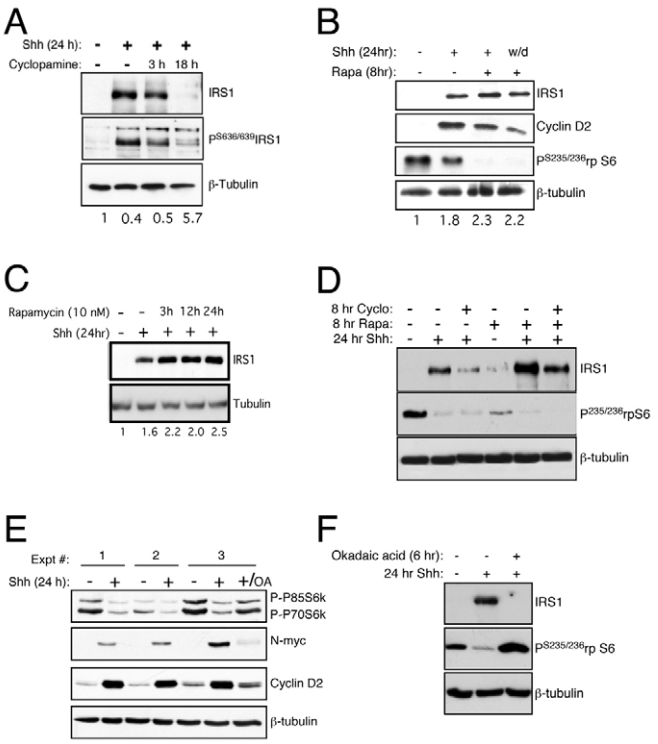

Fig. 3. SHH signaling inhibits S6 kinase activation and hence IRS1 degradation. (**A**) Treatment of CGNPs with 1 μg/ml cyclopamine after increasing periods of time reduced IRS1 protein levels and increased detectable phosphorylated IRS1. The value under each lane represents the ratio of phosphorylated IRS1 to IRS1 as measured by densitometry. (**B**) CGNPs were treated with SHH and/or 10 nm rapamycin (Rapa) as indicated. The final lane represents CGNPs from which SHH was removed at the time of rapamycin addition. Rapamycin in combination with SHH causes an accumulation of IRS1 and rapamycin prevents reduction in IRS1 when SHH is removed. The value under each lane represents densitometric measurement of the IRS1 signal using the vehicle:tubulin value set to 1. (**C**) Treatment of CGNPs with rapamycin in the presence of SHH caused an accumulation of IRS1 over time. The value under each lane represents densitometric measurement of the IRS1 signal using the vehicle:tubulin value set to 1. (**D**) SHH, cyclopamine and rapamycin were given to CGNPs, as indicated above the lanes. Cyclopamine caused reduction in IRS1 levels, whereas rapamycin caused additional IRS1 accumulation in the presence of SHH. Rapamycin partially rescued the cyclopamine-mediated reduction of IRS1 in SHH-treated cells. (**E**) Treatment with SHH reduces the phosphorylation of S6K and hence its activation. Inhibition of PP2A with okadaic acid (OA, 100 nM) restores S6K activation and reduces N-myc as well as cyclin D2 levels in CGNPs. (**F**) Treatment with OA restores S6 phosphorylation and reduces IRS1 levels even in the presence of SHH.

that synergize with GLI1 to achieve the full IRS1 accumulation response to exogenous SHH signaling. Future studies will determine whether GLI affects IRS1 stability and/or mRNA translation, and will identify non-GLI mediators of IRS1 accumulation.

SHH signaling stabilizes IRS1 by downregulating S6 kinase

Several signaling proteins have been shown to play roles in IRS1 degradation, including suppressor of cytokine signaling (SOCS) signaling, retinoic-acid mediated protein kinase C activation, and mTOR, which mediates IRS1 phosphorylation on $S^{636/639}$, to promote its degradation (del Rincon et al., 2004; Haruta et al., 2000; Ishizuka et al., 2007; Shah and Hunter, 2006). As CGNPs are not cultured in the presence of cytokines or retinoic acid, we asked whether SHH signaling affected mTOR-regulated IRS1 turnover by reducing IRS1 phosphorylation and/or activity of S6 kinase, the mTOR substrate shown to directly phosphorylate IRS1 (Shah and Hunter, 2006). We treated CGNPs with SHH and cyclopamine for increasing periods of time, and then carried out western blot analysis for total IRS1 and $S^{636/639}$-phosphorylated IRS1. As expected, IRS1 protein levels declined over time in the presence of cyclopamine (Fig. 3A). However, the ratio of $P^{S636/639}$IRS1 to total IRS1 increases, indicating SHH inhibition increases IRS1 phosphorylation on this destabilization-associated site.

IRS1 phosphorylation on $S^{636/639}$ occurs downstream of mTOR in 293HEK cells (Tzatsos and Kandror, 2006). In order to determine whether mTOR signaling has an affect on IRS1 protein levels in response to SHH, we treated CGNPs with rapamycin, a compound that inhibits the mTOR:Raptor complex, in the presence of or after the withdrawal of SHH. Consistent with previous reports (Hartley and Cooper, 2002), we observed that in the presence of rapamycin, IRS1 levels accumulated (Fig. 3B,C) without any affect on cell survival based on activated caspase 3 levels (data not shown). Interestingly, levels of IRS1 were stabilized after treatment with rapamycin, even when SHH was removed at the time of rapamycin addition (Fig. 3B, lane 4). This suggests that inhibiting mTOR can promote IRS1 stabilization in CGNPs. To further investigate the relationship between SHH signaling and the mTOR

pathway, we treated CGNPs with cyclopamine and rapamycin, and examined IRS1 levels. Although treatment with rapamycin increased IRS levels compared with SHH alone, we observed only partial recovery of IRS1 protein when CGNPs were treated with cyclopamine and rapamycin (Fig. 3D). This result suggests that inhibition of mTOR is not the sole mechanism through which SHH mediates IRS1 accumulation. For example, SHH may also regulate *Irs1* mRNA translation in an mTOR-independent manner. The results may also indicate that mTOR is regulated in part by signaling through SMO.

S6K1, a major target of mTOR, is required for IRS1 phosphorylation in cells and can also directly phosphorylate IRS1 (Easton et al., 2006; Um et al., 2004). Stabilization of IRS1 protein in CGNPs after treatment with rapamycin could occur directly by the inhibition of mTOR or indirectly by inhibiting S6K1, the downstream target of mTOR. As both mTOR and S6K1 can phosphorylate IRS1, we wanted to determine the affects of SHH on the activation of S6K. Western blot analysis (Fig. 3E) shows that S6K phosphorylation, an indicator of its activation by mTOR, is reduced in SHH-treated CGNPs. Consistent with reduced S6K activity in SHH-treated CGNPs, we also observed reduced phosphorylation of the S6K substrate ribosomal protein S6 in SHH-treated CGNPs (Fig. 3B,D).

S6K de-phosphorylation is mediated by protein phosphatase 2A (Peterson et al., 1999; Petritsch et al., 2000), a positive regulator of N-myc stability (Sjostrom et al., 2005) and we can inhibit PP2A by the addition of okadaic acid (OA). As expected, PP2A inhibition destabilized N-Myc (Fig. 3E) (Sjostrom et al., 2005). OA treatment also rescued S6K phosphorylation in the presence of SHH (Fig. 3E, final lane). In addition, OA treatment not only rescues S6K activity, as determined by phosphorylation of its substrate ribosomal protein S6, but it also blocks SHH-mediated IRS1 stabilization (Fig. 3F). These results suggest that SHH signaling inhibits S6K1 activity, thereby promoting stabilization of IRS1 protein.

Alteration of IRS1 levels modulates CGNP proliferation in vitro

To investigate a role for IRS1 in CGNP proliferation, we used lentiviruses expressing small hairpin RNAs (shRNAs) targeting IRS1. We found that of six shRNAs tested by transfection into a murine cell line, all six effectively knocked down IRS1 (data not shown). SHH-treated CGNPs infected with pooled lentiviruses expressing shRNA against IRS1 had reduced IRS1 protein levels (Fig. 4A). We did not observe compensatory upregulation of IRS2, nor did we detect effects of IRS1 knock down on other members of the IGF pathway (Fig. 4A). Consistent with results shown in Fig. 1, neither SHH treatment nor IRS1 knockdown affected AKT phosphorylation. However, levels of cyclin D2 are decreased in response to shRNA treatment, suggesting that reduction of IRS1 protein affects cell cycle progression (Fig. 4A).

To determine whether shRNA-mediated IRS1 knock down impairs CGNP proliferation, we first assayed these viruses on PN5 cerebellar slices. We infected 300 μm cerebellar sections with IRS1 shRNA lentiviruses, then treated the slices with medium containing SHH or SHH vehicle ('SHH–'). After 48 hours, the sections were pulsed with BrdU for 4 hours, fixed, sectioned and stained for BrdU incorporation. Treatment with exogenous SHH increases levels of BrdU incorporation (Fig. 4B, right panels) as well as EGL thickness as previously reported (Wechsler-Reya and Scott, 1998). Infection of the slice cultures with shRNA lentiviruses in conjunction with SHH leads to reduced BrdU staining (Fig. 4B, bottom right panel).

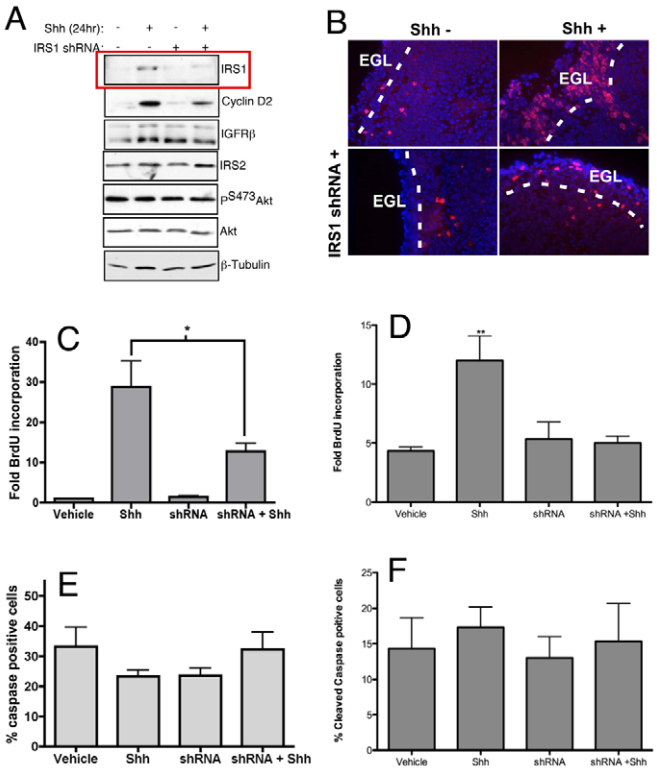

Fig. 4. IRS1 is necessary to maintain CGNP proliferation. (**A**) CGNPs were treated with SHH for 24 hours prior to infection with IRS1 shRNAs for 3 hours at which time the medium was replaced with either SHH treated or untreated medium. Treatment with shRNAs knocked down levels of IRS1 (red box) as well as levels of cyclin D2 without affecting the activation of AKT or levels of IRS2. β-Tubulin confirms equal loading. (**B**) Infection of cerebellar slices with lentiviruses targeting IRS1 causes reduced thickness of the EGL (broken white lines) and reduced BrdU incorporation (red) in the EGL. Blue represents DAPI counterstaining. (**C**) Levels of proliferation in primary CGNP cultures in response to IRS1 shRNA lentivirus infection were determined by measuring BrdU incorporation after a 2-hour BrdU pulse. Reduced BrdU incorporation is evident in shRNA plus SHH compared with SHH-treated CGNPs. BrdU-positive cells were counted and values expressed as percent of total cells per field. Values are represented as fold BrdU-positive cells over untreated CGNPs. *P<0.05, n=4. (**D**) Levels of BrdU incorporation were assessed as above in Percoll gradient-purified CGNP cultures. Trends of BrdU incorporation remain the same as mixed cultures. **P<0.01. (**E**) Cell survival was assessed by immunostaining for cleaved caspase 3. Based on quantification of cleaved caspase 3-positive cells, there was no change in cell survival regardless of treatment. (**F**) Cell survival in response to shRNA treatment remained the same in purified cultures. Cleaved caspase 3-positive cells were counted and values are expressed as percent of total cells per field. Error bars represent s.e.m., n=5.

Importantly, changes in proliferation in response to SHH and/or shRNA lentiviurus occurred in the EGL where CGNPs reside during their proliferation phase.

To quantify the effects of shRNA treatment on proliferation, we measured BrdU incorporation in control or shRNA lentivirus-infected dissociated CGNPs. Forty-eight hours after infection, the CGNPs were pulsed with BrdU for 2 hours prior to fixation and immunofluorescent stained for BrdU incorporation or the proliferation marker Ki67 (see Fig. S4 in the supplementary material). We found a significant reduction in BrdU-positive cells

in SHH-treated CGNPs infected with shRNA lentiviruses targeting IRS1 compared with SHH-treated alone (Fig. 4C). To confirm that effects of IRS1 knock down are specifically attributed to CGNPs, Percoll purified cultures comprising 98% CGNPs were treated with shRNAs with or without SHH. As in the mixed culture system, there was a significant decrease in proliferation after exposure to IRS1-specific shRNAs (Fig. 4D). CGNPs infected with lentiviruses targeting GFP did not show reduced proliferation (see Fig. S4D in the supplementary material). Vehicle-treated cells did not proliferate under any conditions. These results demonstrate that IRS1 is a crucial mediator of SHH-mediated CGNP proliferation.

IGF-induced PI-3K and AKT activation are essential for neuronal survival (Dudek et al., 1997). Although we do not see changes in the activation of AKT in response to SHH (Fig. 1A) or with treatment with IRS1 shRNA (Fig. 4A), knock down of IRS1 may still impact CGNP survival. To determine whether proliferation decreases in IRS1 knock down CGNPs reflect compromised survival, we performed immunostaining for cleaved caspase 3. Knock down of IRS1 in the presence or absence of SHH did not affect cell survival in mixed or Percoll purified cultures (Fig. 4E,F; see Fig. S4 in the supplementary material), suggesting that the function of IRS1 in CGNPs promotes proliferation and not cell survival.

In order to determine whether IRS1 overexpression can maintain CGNP proliferation in the absence of SHH, we infected CGNPs with a retrovirus expressing IRS1. Ectopic expression of IRS1 in CGNPs did not result in alteration of other members of the IGF pathway (Fig. 5A). Ectopic IRS1 expression in SHH-treated cells did not result in increased cyclin D2 levels. However, we observed that overexpression of IRS1 maintained cyclin D2 expression when SHH was removed (Fig. 5A). To determine whether IRS1-driven cyclin D2 expression in the absence of exogenous SHH is associated with activation of intracellular SHH pathway components, we assayed expression levels of *Gli1* and *Gli2*. As shown in Fig. 5B, RT-PCR analysis of these transcription factors demonstrates that IRS1 does not induce their expression. However, expression of *N-myc*, a well-characterized SHH signaling target (Kenney et al., 2003), is increased in response to IRS1 overexpression. These results suggest that SHH-mediated activation of N-myc may be a result of IRS1 stabilization, and that IRS1 does not act upstream of GLI1.

We next determined the effect of IRS1 expression on CGNP proliferation by staining BrdU-pulsed CGNPs infected with IRS1-expressing retroviruses. We see an increase in BrdU staining as well as increased Ki67, a proliferation marker, in SHH-treated CGNPs compared with untreated cells as expected (see Fig. S5A in the supplementary material). Ki67 expression is maintained in the absence of SHH when cells are infected with IRS1-expressing retrovirus before SHH withdrawal. To confirm these results and to quantify the affects of IRS1 expression on proliferation, CGNPs were pulsed with BrdU as described. CGNPs from which SHH was removed after infection with IRS1 have significantly more BrdU incorporation compared with untreated alone (Fig. 5C). Similar results were obtained with IRS1-infected SHH-treated cells were exposed to cyclopamine, indicating that IRS1 effects on CGNP proliferation are Smoothened independent (data not shown). However, in comparison with SHH-treated, non-IRS1-infected CGNPs, BrdU incorporation is reduced, indicating that other components of the SHH signaling pathway are necessary to maintain full CGNP proliferation in vitro. Treatment of IRS1-infected CGNPs with cyclopamine yielded similar results

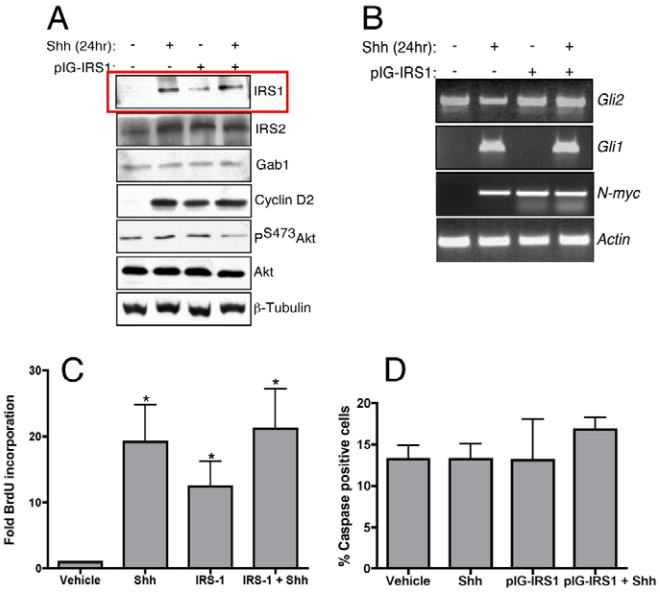

Fig. 5. IRS1 overexpression maintains CGNP proliferation in the absence of SHH. CGNPs were treated with SHH for 24 hours prior to infection with retrovirus expressing IRS1. (**A**) Western blotting shows that IRS1 overexpression maintains increased levels of cyclin D2 after SHH withdrawal. (**B**) RT-PCR analysis shows no effect of IRS1 overexpression on GLI1 or GLI2 expression, but did show an increase in N-myc expression. (**C**) Levels of CGNP proliferation in response to IRS1-expressing retrovirus infection were assessed with BrdU incorporation. Numbers of BrdU-positive cells are increased with treatment of SHH, as well as treatment with IRS1 retrovirus. Quantification of BrdU incorporation was performed as described in Fig. 4D. (**D**) To assess effects of virus treatment on cell death CGNPs were stained with antibodies to activated caspase 3. Levels of cleaved caspase 3 remain the same for all treatment groups. Cleaved caspase 3-positive cells were counted and values are expressed as percent of total cells per field. Error bars represent s.e.m., n=5. Asterisks indicate statistically significant difference to untreated CGNPs (P<0.05, n=4).

(data not shown), indicating that sustained proliferation in IRS1-infected, SHH withdrawn CGNPs is not a result of residual SHH in the medium.

The increase in proliferation levels in IRS1 overexpressing, non-SHH-treated cells does not appear to result from a cell survival advantage as levels of activated caspase 3 remain the same in all treatment groups (Fig. 5D, see Fig. S5B). Overexpression of IRS1 followed by ongoing SHH treatment did not promote increased proliferation. We speculate that this is because IRS1 is a large scaffolding protein and inducing supra-normal levels may lead to formation of non-functional complexes owing to limiting levels of other components. Taken together, our results suggest that through IRS1 upregulation, the SHH signaling pathway may in effect be hijacking mitogenic effectors of IGF signaling. It is also possible that IRS1 in CGNPs may have additional, IGF-independent functions contributing to proliferation.

IRS1 in SHH-mediated mouse medulloblastoma

Aberrant *IRS1* expression has been associated with several types of cancer, including medulloblastoma (Del Valle et al., 2002; Waters et al., 1993). As we see a role for IRS1 in mediating CGNP proliferation, we looked at IRS1 protein in two mouse models of

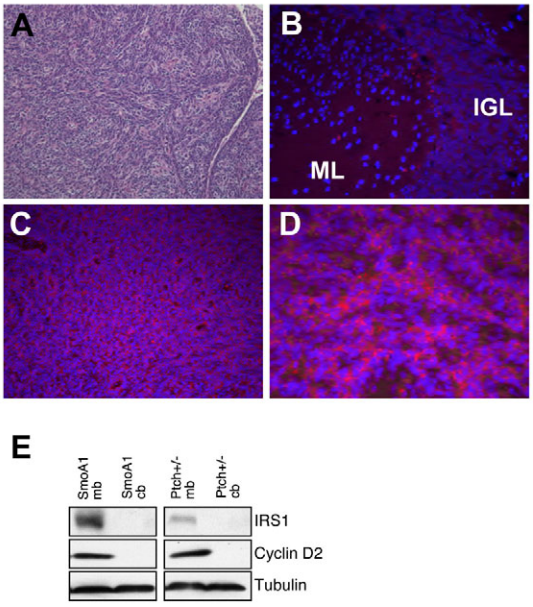

Fig. 6. IRS1 is present in SHH-mediated mouse medulloblastoma. (**A**) Hematoxylin and Eosin staining of a Neuro-D2-SmoA1 medulloblastoma depicts a desmoplastic medulloblastoma. (**B**) Adjacent normal cerebellar areas in the *SmoA1* tumor model show very little IRS1 (red) immunostaining. (**C**,**D**) Increased IRS1 protein can be seen within the tumor at both 10× (C) and 63× (D) magnification (blue=DAPI). (**E**) Western blot analysis for both *Ptch1*$^{+/-}$ and *SmoA1* medulloblastoma models show increased IRS1 expression coinciding with increased cyclin D2 expression. IGL, internal granule layer; ML, molecular layer.

medulloblastoma. Both the *Ptch1*$^{+/-}$ and Neuro-D2-SmoA1 mice form spontaneous medulloblastoma as a result of aberrant activation of the SHH signaling pathway (Berman et al., 2002; Goodrich et al., 1997; Hallahan et al., 2004). We found that tumors in both mice strains showed elevated IRS1 levels compared with adjacent normal brain tissue (Fig. 6 and data not shown). Tumor lysates from these mice also show increased IRS1 levels compared with non-tumor cerebellar tissue, which correlates with increased cyclin D2 levels (Fig. 6E).

DISCUSSION

Normal CGNP proliferation is dependent upon SHH and IGF signaling, and both signaling pathways are implicated in medulloblastoma, a brain tumor for which CGNPs are a proposed cell of origin. We found that SHH specifically upregulates the IGF receptor-interacting scaffolding protein IRS1 without altering levels of other members of the IGF pathway, including IRS2, GAB1 or activated AKT. Furthermore, IRS1 protein levels depend upon constant SHH signaling in vitro and IRS1 is found in proliferating CGNPs in vivo, suggesting that IRS1 appears at the right time and place to play roles in SHH-dependent CGNP proliferation. IRS1 protein is also seen in mouse medulloblastoma in conjunction with high levels of cyclin D2 expression, suggesting that IRS1 may also be playing a role in disease. Such a role for IRS1 is supported by our experiments showing that IRS1 overexpression in CGNPs is capable of sustaining proliferation even in the absence of SHH, whereas knock down of IRS1 blocks proliferation in the presence of SHH.

In cell lines, it has been shown that IRS1 stability can be regulated by a negative-feedback loop wherein S6K1 phosphorylates IRS1, targeting it for degradation by the proteasome (Easton et al., 2006). We observed that this feedback loop exists in primary CGNP cultures, and that SHH interferes with this process by suppressing S6 kinase activity, thereby stabilizing IRS1. Our results indicate that SHH suppresses S6 kinase activity by inhibiting its upstream regulator mTOR. Two previous studies have indicated interactions between the mTOR pathway and the hedgehog pathway, in that mTOR can regulate Indian hedgehog levels in chondrocytes and that mTOR inhibition impairs survival in epitheloid cells overexpressing GLI1 (Phornphutkul et al., 2008; Louro et al., 1999). These studies did not investigate how SHH signaling affects mTOR activity in primary neurons. Our data indicate that SHH-mediated mTOR inhibition is to some extent dependent upon Smoothened signaling, but the inability of cyclopamine to completely rescue S6K activity indicates existence of additional mechanisms. IRS1 regulation by stabilization instead of increased transcription has been reported in other cell types (Lee et al., 2003; Nemoto et al., 2006; Renstrom et al., 2005), but not in the setting of SHH signaling. Our study indicates a role for SHH-mediated IRS1 mRNA translation in addition to its stabilization in proliferating CGNPs.

In addition to regulating IRS1 stability, SHH may also affect IRS1 mRNA translation, as the mRNA for IRS1 is present in untreated CGNPs but the protein is not detectable, even upon the addition of lactacystin. The determine whether SHH influences loading of IRS1 mRNA onto polysomes in CGNPs will be of future interest when techniques have evolved to make this experiment feasible. Currently, our results are consistent with a role for IGF signaling through AKT to promote survival (Dudek et al., 1997; Miller et al., 1997), coincident with stabilization of N-myc through GSK3β (Kenney et al., 2004). In the absence of SHH signaling, IGF signaling activates the PI-3K pathway, leading to neuronal survival (Fig. 7). As levels of the IGF effectors IRS2 and GAB1 are

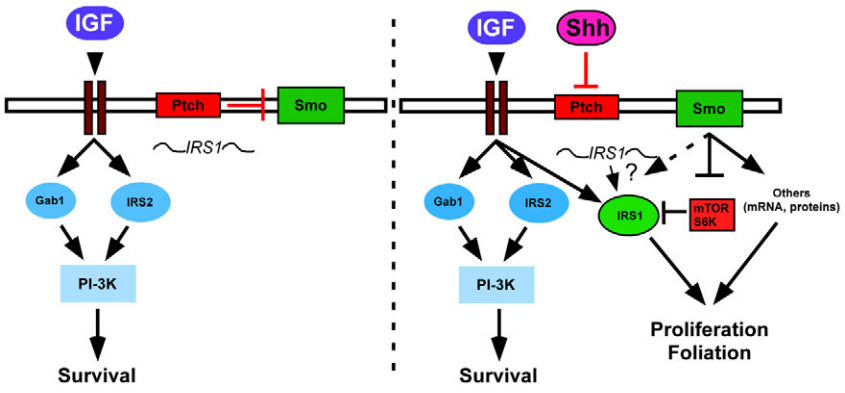

Fig. 7. Model suggesting how SHH mediates IRS1 expression during CGNP proliferation. In the absence of SHH, IGF signaling sends survival cues through IRS2 and/or GAB1 and PI-3K signaling (left panel). IRS1 mRNA is present. In the presence of SHH, IRS1 is upregulated by a mechanism that may involve both enhanced translation and protein stabilization. SHH stabilizes IRS1 protein by inhibiting mTOR-mediated activation of S6K, which is known to phosphorylate IRS1 leading to its degradation.

unchanged in response to SHH, IGF survival signals may proceed through these signaling molecules and not IRS1. In the presence of SHH, IGF signaling continues to send survival signals but can now also exert mitogenic effects through newly translated, stabilized IRS1, along with other factors important in mediating CGNP proliferation, such as N-myc (Fig. 7) (Kenney et al., 2003).

Our results demonstrate a role for IRS1 in mediating CGNP proliferation, and thus IRS1 may have a role in cell cycle progression in medulloblastoma. It has been shown that overexpression of IRS1 is sufficient to mediate transformation of mouse fibroblasts (D'Ambrosio et al., 1995). IRS1 has been found to have a role in several types of cancer, including breast cancer, while the IGF pathway has been strongly linked to medulloblastoma (Dearth et al., 2007; Dearth et al., 2006; Del Valle et al., 2002; Rao et al., 2004). One group has reported IRS1 expression in a JC-virus-induced mouse medulloblastoma (Khalili et al., 2003), but a relationship between IRS1 and SHH-mediated medulloblastoma has not been reported. We report overexpression of IRS1 in two models of mouse SHH-induced medulloblastoma. This makes IRS1 an attractive candidate as a potential target for cancer therapies.

How IRS1 mediates CGNP proliferation remains unclear. Our data suggest that the effects of IRS1 do not occur through the activity of PI-3K. One possibility is that IRS1 increases CGNP survival by interacting with Bcl2 (Ueno et al., 2000); however, modulation of IRS1 levels in vitro do not alter cell survival, making this scenario unlikely. Recent studies in mammary tumors suggest that IRS1 interacts with proteins with known roles in proliferation, such as β-catenin (Dearth et al., 2006). It remains to be determined whether this occurs in CGNPs and SHH-derived medulloblastomas. It is also possible that IRS1, a large scaffolding protein, has unknown interactors in SHH-stimulated CGNPs. Future studies exploring the specific mechanism through which IRS1 promotes SHH-stimulated CGNP proliferation may also identify novel targets for development of new treatments for medulloblastoma and other cancers.

We thank the Sontag Foundation and Alex's Lemonade Stand Foundation for supporting these studies. This work was also supported by NIH 1R01NS061070-01 (A.M.K.) and NRSA fellowship F32AG030888 (S.P.). A.F.-L receives fellowship support from the Spanish Ministry of Education. The contents of this manuscript are the sole responsibility of the authors and do not necessarily represent the official views of the NINDS, the NIA, the Sontag Foundation or Alex's Lemonade Stand Foundation. We thank Tim Gershon for assistance with generating IRS1 retroviruses, and we thank William Hahn for advice concerning use of shRNA lentiviruses.

Supplementary material

Supplementary material for this article is available at http://dev.biologists.org/cgi/content/full/135/19/3291/DC1

References

Alcedo, J., Ayzenzon, M., Von Ohlen, T., Noll, M. and Hooper, J. E. (1996). The Drosophila smoothened gene encodes a seven-pass membrane protein, a putative receptor for the hedgehog signal. *Cell* **86**, 221-232.

Altman, J. and Bayer, S. (1997). *Development of the Cerebellar System in Relation to its Evolution, Structure, and Functions.* Boca Raton, FL, USA: CRC Press.

Aruga, J., Inoue, T., Hoshino, J. and Mikoshiba, K. (2002). Zic2 controls cerebellar development in cooperation with Zic1. *J. Neurosci.* **22**, 218-225.

Berman, D. M., Karhadkar, S. S., Hallahan, A. R., Pritchard, J. I., Eberhart, C. G., Watkins, D. N., Chen, J. K., Cooper, M. K., Taipale, J., Olson, J. M. et al. (2002). Medulloblastoma growth inhibition by hedgehog pathway blockade. *Science* **297**, 1559-1561.

Cai, D., Shen, Y., De Bellard, M., Tang, S. and Filbin, M. T. (1999). Prior exposure to neurotrophins blocks inhibition of axonal regeneration by MAG and myelin via a cAMP-dependent mechanism. *Neuron* **22**, 89-101.

Chen, J. K., Taipale, J., Young, K. E., Maiti, T. and Beachy, P. A. (2002). Small molecule modulation of Smoothened activity. *Proc. Natl. Acad. Sci. USA* **99**, 14071-14076.

Chen, J., Wu, A., Sun, H., Drakas, R., Garofalo, C., Cascio, S., Surmacz, E. and Baserga, R. (2005). Functional significance of type 1 insulin-like growth factor-mediated nuclear translocation of the insulin receptor substrate-1 and beta-catenin. *J. Biol. Chem.* **280**, 29912-29920.

Corrales, J. D., Rocco, G. L., Blaess, S., Guo, Q. and Joyner, A. L. (2004). Spatial pattern of sonic hedgehog signaling through Gli genes during cerebellum development. *Development* **131**, 5581-5590.

Corrales, J. D., Blaess, S., Mahoney, E. M. and Joyner, A. L. (2006). The level of sonic hedgehog signaling regulates the complexity of cerebellar foliation. *Development* **133**, 1811-1821.

D'Ambrosio, C., Keller, S., Morrione, A., Lienhard, G., Baserga, R. and Surmacz, E. (1995). Transforming potential of the insulin receptor substrate 1. *Cell Growth Differ.* **6**, 557-562.

Dahmane, N. and Ruiz-i-Altaba, A. (1999). Sonic hedgehog regulates the growth and patterning of the cerebellum. *Development* **126**, 3089-3100.

Dearth, R. K., Cui, X., Kim, H.-J., Kuiatse, I., Lawrence, N. A., Zhang, X., Divisova, J., Britton, O. L., Mohsin, S., Allred, D. C. et al. (2006). Mammary tumorigenesis and metastasis caused by overexpression of insulin receptor substrate 1 (IRS-1) or IRS-2. *Mol. Cell. Biol.* **26**, 9302-9314.

Dearth, R., Cui, X., Kim, H., Hadsell, D. and Lee, A. (2007). Oncogenic transformation by the signaling adaptor proteins insulin receptor substrate (IRS)-1 and IRS-2. *Cell Cycle* **6**, 705-713.

del Rincon, S., Guo, Q., Morelli, C., Shiu, H., Surmacz, E. and Miller, W. J. (2004). Retinoic acid mediates degradation of IRS1 by the ubiquitin-proteasome pathway, via a PKC-dependant mechanism. *Oncogene* **23**, 9269-9279.

Del Valle, L., Enam, S., Lassak, A., Wang, J. Y., Croul, S., Khalili, K. and Reiss, K. (2002). Insulin-like growth factor I receptor activity in human medulloblastomas. *Clin. Cancer Res.* **8**, 1822-1830.

Dudek, H., Datta, S. R., Franke, T. F., Birnbaum, M. J., Yao, R., Cooper, G. M., Segal, R. A., Kaplan, D. R. and Greenberg, M. E. (1997). Regulation of neuronal survival by the serine-threonine protein kinase Akt. *Science* **275**, 661-665.

Easton, J. B., Kurmasheva, R. T. and Houghton, P. J. (2006). IRS-1: Auditing the effectiveness of mTOR inhibitors. *Cancer Cell* **9**, 153-155.

Goodrich, L. V., Milenkovic, L., Higgins, K. M. and Scott, M. P. (1997). Altered neural cell fates and medulloblastoma in mouse patched mutants. *Science* **277**, 1109-1113.

Hahn, H., Wojnowski, L., Specht, K., Kappler, R., Calzada-Wack, J., Potter, D., Zimmer, A., Muller, U., Samson, E. and Quintanilla-Martinez, L. (2000). Patched target Igf2 is indispensable for the formation of medulloblastoma and rhabdomyosarcoma. *J. Biol. Chem.* **275**, 28341-28344.

Hallahan, A. R., Pritchard, J. I., Hansen, S., Benson, M., Stoeck, J., Hatton, B. A., Russell, T. L., Ellenbogen, R. G., Bernstein, I. D., Beachy, P. A. et al. (2004). The SmoA1 mouse model reveals that Notch signaling is critical for the growth and survival of Sonic Hedgehog-induced medulloblastomas. *Cancer Res.* **64**, 7794-7800.

Hartley, D. and Cooper, G. M. (2002). Role of mTOR in the degradation of IRS-1: Regulation of PP2A activity. *J. Cell. Biochem.* **85**, 304-314.

Hartmann, W., Koch, A., Brune, H., Waha, A., Schuller, U., Dani, I., Denkhaus, D., Langmann, W., Bode, U., Wiestler, O. D. et al. (2005). Insulin-like growth factor II is involved in the proliferation control of medulloblastoma and its cerebellar precursor cells. *Am. J. Pathol.* **166**, 1153-1162.

Haruta, T., Uno, T., Kawahara, J., Takano, A., Egawa, K., Sharma, P. M., Olefsky, J. M. and Kobayashi, M. (2000). A rapamycin-sensitive pathway down-regulates insulin signaling via phosphorylation and proteasomal degradation of insulin receptor substrate-1. *Mol. Endocrinol.* **14**, 783-794.

Hatten, M. and Heintz, N. (1995). Mechanisms of neural patterning and specification in the developing cerebellum. *Annu. Rev. Neurosci.* **18**, 385-408.

Ho, K. S. and Scott, M. P. (2002). Sonic hedgehog in the nervous system: functions, modifications and mechanisms. *Curr. Opin. Neurobiol.* **12**, 57-63.

Ishizuka, K., Usui, I., Kanatani, Y., Bukhari, A., He, J., Fujisaka, S., Yamazaki, Y., Suzuki, H., Hiratani, K., Ishiki, M. et al. (2007). Chronic tumor necrosis factor-alpha treatment causes insulin resistance via insulin receptor substrate-1 serine phosphorylation and suppressor of cytokine signaling-3 induction in 3T3-L1 adipocytes. *Endocrinology* **148**, 2994-3003.

Kenney, A. M. and Rowitch, D. H. (2000). Sonic hedgehog promotes G(1) cyclin expression and sustained cell cycle progression in mammalian neuronal precursors. *Mol. Cell. Biol.* **20**, 9055-9067.

Kenney, A. M., Cole, M. D. and Rowitch, D. H. (2003). Nmyc upregulation by sonic hedgehog signaling promotes proliferation in developing cerebellar granule neuron precursors. *Development* **130**, 15-28.

Kenney, A. M., Widlund, H. R. and Rowitch, D. H. (2004). Hedgehog and PI-3 kinase signaling converge on Nmyc1 to promote cell cycle progression in cerebellar neuronal precursors. *Development* **131**, 217-228.

Khalili, K., Del Valle, L., Wang, J. Y., Darbinian, N., Lassak, A., Safak, M. and Reiss, K. (2003). T-antigen of human polyomavirus JC cooperates with IGF-IRS singaling system in cerebellar tumors of the childhood-medulloblastomas. *Anticancer Res.* **23**, 2035-2041.

Knoepfler, P. and Kenney, A. (2006). Neural precursors cycling at sonic speed: N-Myc pedals, GSK-3 breaks. *Cell Cycle* **5**, 47-52.
Lee, A. V., Gooch, J. L., Oesterreich, S., Guler, R. L. and Yee, D. (2000). Insulin-like growth factor I-induced degradation of insulin receptor substrate 1 is mediated by the 26S proteasome and blocked by phosphatidylinositol 3′-kinase inhibition. *Mol. Cell. Biol.* **20**, 1489-1496.
Lee, A. V., Zhang, P., Ivanova, M., Bonnette, S., Oesterreich, S., Rosen, J. M., Grimm, S., Hovey, R. C., Vonderhaar, B. K., Kahn, C. R. et al. (2003). Developmental and hormonal signals dramatically alter the localization and abundance of insulin receptor substrate proteins in the mammary gland. *Endocrinology* **144**, 2683-2694.
Louro, I. D., McKie-Bell, P., Gosnell, H., Brindley, B. C., Bucy, R. P. and Ruppert, J. M. (1999). The zinc finger protein GLI induces cellular sensitivity to the mTOR inhibitor rapamycin. *Cell Growth Differ.* **10**, 503-516.
Marino, S. (2005). Medulloblastoma: developmental mechanisms out of control. *Trends Mol. Med.* **11**, 17-22.
Mill, P., Mo, R., Hu, M. C., Dagnino, L., Rosenblum, N. D. and Hui, C. C. (2005). Shh controls epithelial proliferation via independent pathways that converge on N-Myc. *Dev. Cell* **9**, 293-303.
Miller, T. M., Tansey, M. G., Johnson, E. M., Jr and Creedon, D. J. (1997). Inhibition of phosphatidylinositol 3-kinase activity blocks depolarization- and insulin-like growth factor I-mediated survival of cerebellar granule cells. *J. Biol. Chem.* **272**, 9847-9853.
Morelli, C., Garofalo, C., Sisci, D., del Rincon, S., Cascio, S., Tu, X., Vecchione, A., Sauter, E. R., Miller, W. H., Jr and Surmacz, E. (2004). Nuclear insulin receptor substrate 1 interacts with estrogen receptor alpha at ERE promoters. *Oncogene* **23**, 7517-7526.
Nemoto, T., Yokoo, H., Satoh, S., Yanagita, T., Sugano, T., Yoshikawa, N., Maruta, T., Kobayashi, H. and Wada, A. (2006). Constitutive activity of glycogen synthase kinase-3B: Positive regulation of steady-state levels of insulin receptor substrates-1 and -2 in adrenal chromaffin cells. *Brain Res.* **1110**, 1-12.
Oliver, T. G., Grasfeder, L. L., Carroll, A. L., Kaiser, C., Gillingham, C. L., Lin, S. M., Wickramasinghe, R., Scott, M. P. and Wechsler-Reya, R. J. (2003). Transcriptional profiling of the Sonic hedgehog response: a critical role for N-myc in proliferation of neuronal precursors. *Proc. Natl. Acad. Sci. USA* **100**, 7331-7336.
Packer, R. J., Cogen, P., Vezina, G. and Rorke, L. B. (1999). Medulloblastoma: clinical and biologic aspects. *Neurooncology* **1**, 232-250.
Peterson, R. T., Desai, B. N., Hardwick, J. S. and Schreiber, S. L. (1999). Protein phosphatase 2A interacts with the 70-kDa S6 kinase and is activated by inhibition of FKBP12-rapamycinassociated protein. *Proc. Natl. Acad. Sci. USA* **96**, 4438-4442.
Petritsch, C., Beug, H., Balmain, A. and Oft, M. (2000). TGF-beta inhibits p70 S6 kinase via protein phosphatase 2A to induce G(1) arrest. *Genes Dev.* **14**, 3093-3101.
Phornphutkul, C., Wu, K. Y., Auyeung, V., Chen, Q. and Gruppuso, P. A. (2008). mTOR signaling contributes to chondrocyte differentiation. *Dev. Dyn.* **237**, 702-712.
Provias, J. and Becker, L. (1996). Cellular and molecular patholgy of medulloblastoma. *J. Neurooncol.* **29**, 35-43.
Rao, G., Pedone, C. A., Valle, L. D., Reiss, K., Holland, E. C. and Fults, D. W. (2004). Sonic hedgehog and insulin-like growth factor signaling synergize to induce medulloblastoma formation from nestin-expressing neural progenitors in mice. *Oncogene* **23**, 6156-6162.
Reiss, K. (2002). Insulin-like growth factor-I receptor-a potential therapeutic target in medulloblastomas. *Expert. Opin. Ther. Targets* **6**, 539-544.
Renstrom, F., Bruen, J. and Eriksson, J. (2005). Insulin receptor substrates-1 and -2 are both depleted but via different mechanisms after down-regulation of glucose transport in rat adipocytes. *Endocrinology* **146**, 3044-3051.
Rice, M., Turnbow, M. and Garner, C. (1993). Insulin stimulates the degradation of IRS-1 in 3T3-L1 adipocytes. *Biochem. Biophys. Res. Commun.* **190**, 961-967.
Riobo, N. A., Lu, K., Ai, X., Haines, G. M. and Emerson, C. P., Jr (2006). Phosphoinositide 3-kinase and Akt are essential for Sonic Hedgehog signaling. *Proc. Natl. Acad. Sci. USA* **103**, 4505-4510.
Schubert, M., Brazil, D. P., Burks, D. J., Kushner, J. A., Ye, J., Flint, C. L., Farhang-Fallah, J., Dikkes, P., Warot, X. M., Rio, C. et al. (2003). Insulin receptor substrate-2 deficiency impairs brain growth and promotes tau phosphorylation. *J. Neurosci.* **23**, 7084-7092.
Shah, O. and Hunter, T. (2006). Turnover of the active fraction of IRS1 involves raptor-mTOR and S6K1-dependent serine phosphorylation in cell culture models of tuberous sclerosis. *Mol. Cell. Biol.* **26**, 6425-6434.
Sjostrom, S. K., Finn, G., Hahn, W. C., Rowitch, D. H. and Kenney, A. M. (2005). The cdk1 complex plays a prime role in regulating N-myc phosphorylation and turnover in neural precursors. *Dev. Cell* **9**, 327-338.
Tzatsos, A. and Kandror, K. (2006). Nutrients suppress phosphatidylinositol 3-kinase/Akt signaling via raptor-dependent mTOR-mediated insulin receptor substrate 1 phosphorylation. *Mol. Cell. Biol.* **26**, 63-76.
Ueno, H., Kondo, E., Yamamoto-Honda, R., Tobe, K., Nakamoto, T., Sasaki, K., Mitani, K., Furusaka, A., Tanaka, T., Tsujimoto, Y. et al. (2000). Association of insulin receptor substrate proteins with Bcl-2 and their effects on its phosphorylation and antiapoptotic function. *Mol. Biol. Cell* **11**, 735-746.
Um, S. H., Frigerio, F., Watanabe, M., Picard, F., Joaquin, M., Sticker, M., Fumagalli, S., Allegrini, P. R., Kozma, S. C., Auwerx, J. et al. (2004). Absence of S6K1 protects against age- and diet-induced obesity while enhancing insulin sensitivity. *Nature* **431**, 200.
Uziel, T., Zindy, F., Xie, S., Lee, Y., Forget, A., Magdaleno, S., Rehg, J. E., Calabrese, C., Solecki, D., Eberhart, C. G. et al. (2005). The tumor suppressors Ink4c and p53 collaborate independently with Patched to suppress medulloblastoma formation. *Genes Dev.* **19**, 2656-2667.
Van Obberghen, E., Baron, V., Delahaye, L., Emanuelli, B., Filippa, N., Giorgetti-Peraldi, S., Lebrun, P., Mothe-Satney, I., Peraldi, P., Rocchi, S. et al. (2001). Surfing the insulin signaling web. *Eur. J. Clin. Invest.* **31**, 966-977.
Wallace, V. A. (1999). Purkinje-cell-derived Sonic hedgehog regulates granule neuron precursor cell proliferation in the developing mouse cerebellum. *Curr. Biol.* **9**, 445-448.
Waters, S. B., Yamauchi, K. and Pessin, J. E. (1993). Functional expression of insulin receptor substrate-1 is required for insulin-stimulated mitogenic signaling. *J. Biol. Chem.* **268**, 22231-22234.
Wechsler-Reya, R. J. and Scott, M. P. (1999). Control of neuronal precursor proliferation in the cerebellum by Sonic Hedgehog. *Neuron* **22**, 103-114.
Wetmore, C. (2003). Sonic hedgehog in normal and neoplastic proliferation: insight gained from human tumors and animal models. *Curr. Opin. Genet. Dev.* **13**, 34-42.
White, M. (1998). The IRS-signaling system: a network of docking proteins that mediate insulin action. *Mol. Cell. Biochem.* **182**, 3-11.